Electronic Supplementary Material (ESI) for Physical Chemistry Chemical Physics.
This journal is © the Owner Societies 2022

Supplementary information "Intrinsic ferromagnetism and quantum anomalous Hall effect in two-dimensional $MnOCl_2$ monolayers"

Guang Song,[a,*] Chengfeng Zhang,[a] Tengfei Xie,[a] Qingkang Wu,[a] Bingwen Zhang,[b] Xiaokun Huang,[c] Zhongwen Li,[a] Guannan Li,[a] and Benling Gao[a]

[a]*Department of Physics, Huaiyin Institute of Technology, Huaian 223003, China*

[b]*Fujian Key Laboratory of Functional Marine Sensing Materials, Minjiang University, Fuzhou 350108, China*

[c]*School of Materials Science and Engineering, Jingdezhen Ceramic Institute, Jingdezhen 333001, China*

[*] Corresponding author: Guang Song, gsong@hyit.edu.cn;

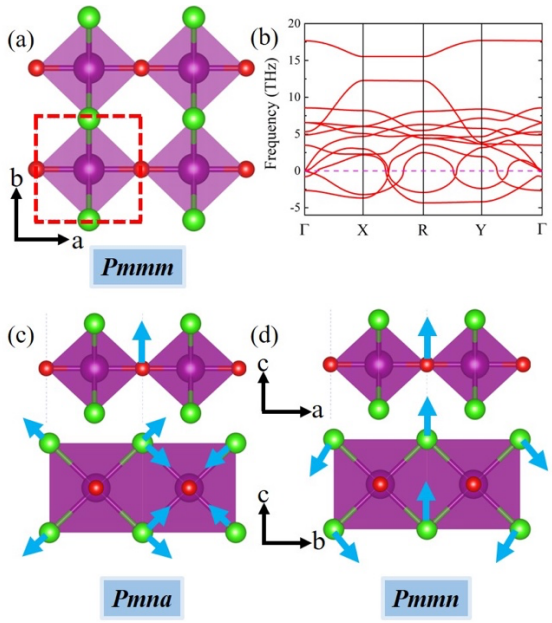

Fig. S1. (a) The schematic of *Pmmm*-$MnOCl_2$ monolayer. (b) The phonon dispersion of Pmmm-$MnOCl_2$ monolayer. (c) and (d) Two different lattice distortions modes according the soft mode in (b). The blue arrows represent the moving directions for different atoms.

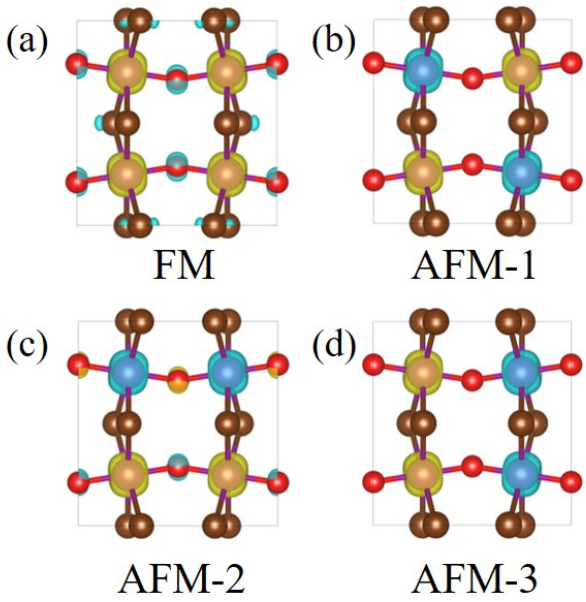

Fig. S2. Spin density isosurfaces of *Pmmn*-$MnOCl_2$ monolayer at the absolute value of $|\Delta\rho| = 0.2$ electrons per $Å^3$ for the four magnetic orders. Yellow and green isosurfaces correspond to positive and negative spin density, respectively.

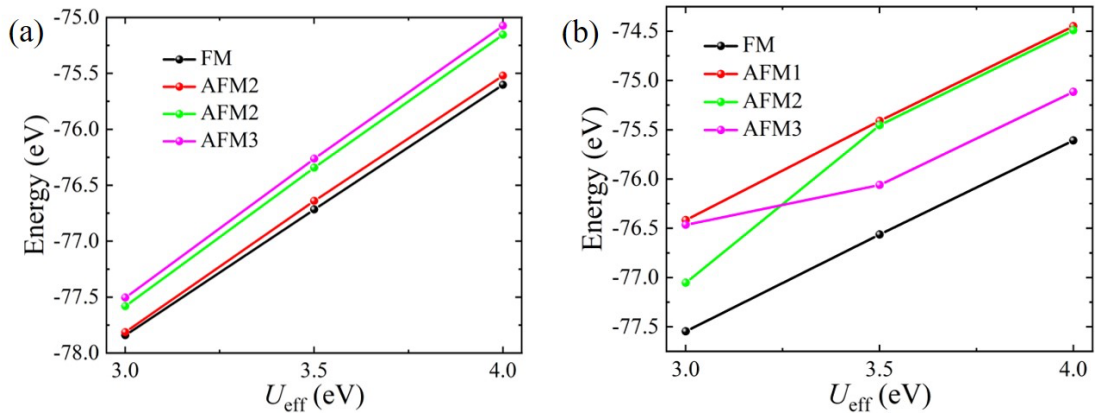

Fig. S3. The calculated total energy of different magnetic ordering as a function of U_{eff}. (a) *Pmna*-$MnOCl_2$. (b) *Pmmn*-$MnOCl_2$.

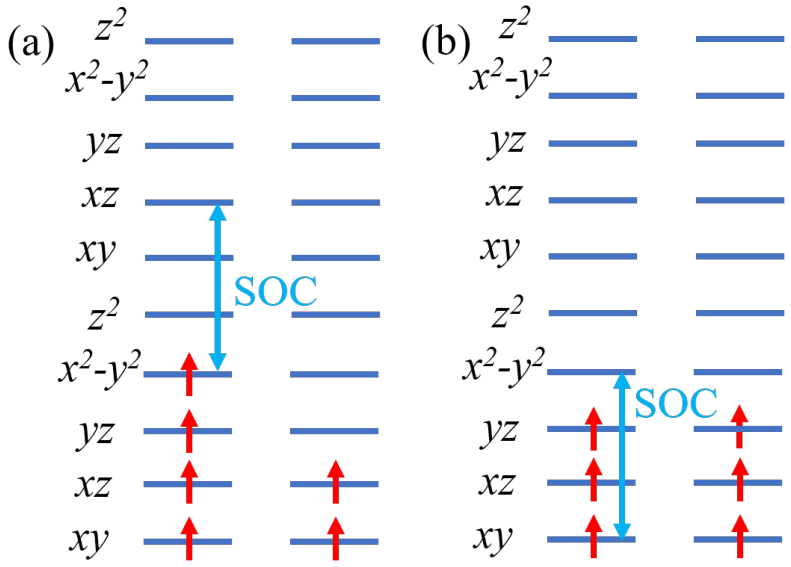

Fig. S4. The orbital structure for $MnOCl_2$ monolayers. (a) *Pmna*-$MnOCl_2$ monolayer. (b) Pmmn-$MnOCl_2$ monolayer.

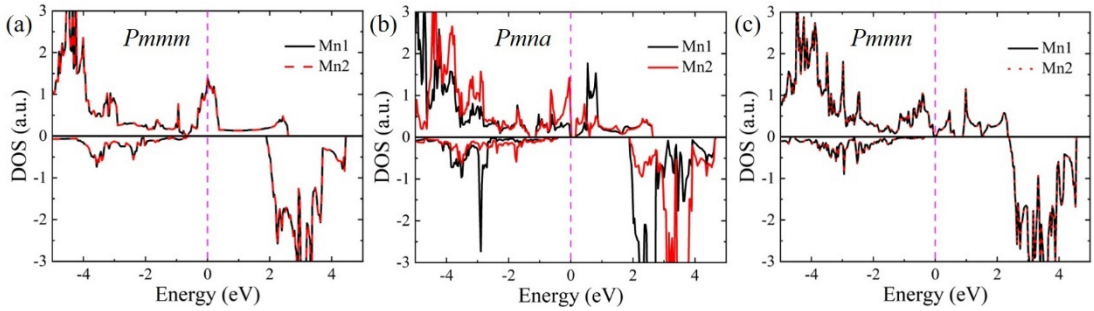

Fig. S5. The calculated density of states for nearest neighbor Mn ions. (a) *Pmmm*-$MnOCl_2$ monolayer. (b) *Pmna*-$MnOCl_2$ monolayer. (c) *Pmmn*-$MnOCl_2$ monolayer.

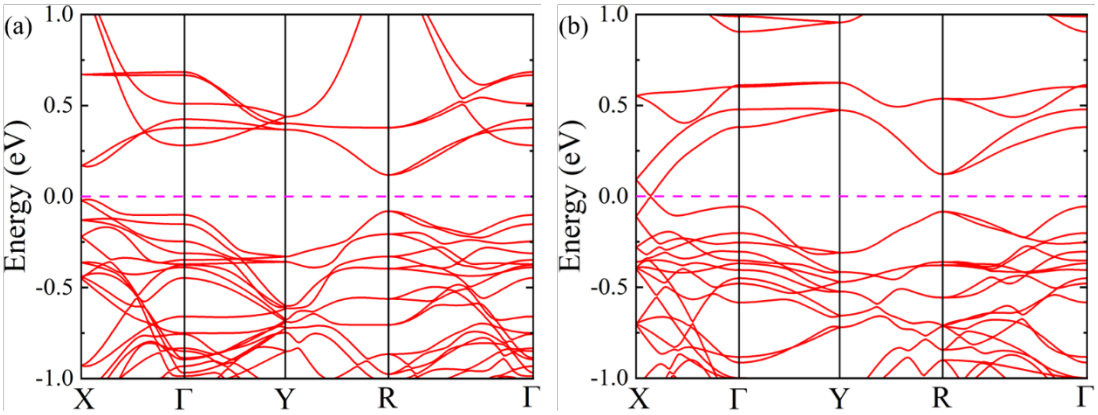

Fig. S6. The calculated bans-structure for *Pmna*-$MnOCl_2$ and *Pmmn* $MnOCl_2$ monolayers. (a) *Pmna*-$MnOCl_2$ monolayer. (b) *Pmmn* $MnOCl_2$ monolayer.

Table S1. The calculated lattice parameter for $MnOCl_2$ monolayers with GGA + *U* method.

	a (Å)	b (Å)	Mn-O (Å)	Mn-Cl (Å)	Mn-O-Mn (°)	Mn-Cl-Mn (°)
Pmmm	3.616	3.499	1.808	2.430	180.00	92.12
Pmna	7.229	7.115	1.795/1.863	2.530/2.324	162.28	94.16
Pmmn	7.067	7.250	1.828	3.645/2.408	150.73	86.50/97.64

Table S2. The calculated total energies of different magnetic ordering and magnetic interactions in $MnOCl_2$ monolayers with GGA + *U* method. The total energy of FM ordering is taken as reference. The unit are in the unit of eV for the total energy and meV for magnetic interaction.

	FM	AFM1	AFM2	AFM3	J_x	J_y	J_{xy}
Pmmm	0.000	0.214	0.058	0.188	-2.326	-0.010	-0.004
Pmna	0.000	0.336	0.028	0.259	-15.76	-2.90	0.67
Pmmn	0.000	1.131	0.495	1.084	-47.77	-15.05	-6.22

Table S3. The calculated energy difference and magnetic interactions for *Pmna*-$MnOCl_2$ monolayer with HSE06 and PBEsol method. The total energy of FM ordering is taken as reference. The unit are in the unit of eV for the total energy and meV for magnetic interaction.

	FM	AFM1	AFM2	AFM3	J_x	J_y	J_{xy}
HSE06	0.000	0.328	0.055	0.256	-14.69	-9.23	0.60
PBEsol	0.000	0.314	0.070	0.253	-13.81	-3.63	-0.13

Table S4. The calculated energy difference and magnetic interactions for *Pmmn*-$MnOCl_2$ monolayer with HSE06 and PBEsol method. The total energy of FM ordering is taken as reference. The unit are in the unit of eV for the total energy and meV for magnetic interaction.

	FM	AFM1	AFM2	AFM3	J_x	J_y	J_{xy}
HSE06	0.000	1.997	1.211	1.557	-65.09	-48.86	-10.69
PBEsol	0.000	1.034	0.495	0.990	-44.28	-13.15	-5.37

Table S5. Matrix elements $|< o|\boldsymbol{S}\cdot\boldsymbol{L}|u >|^2$ of the spin-orbit coupling operator for *d*-orbitals, in units of $\hbar^2$. Spin up and spin down orbits are represented by up and down arrows, respectively.

	$\boldsymbol{d_{xy}}\uparrow$	$\boldsymbol{d_{yz}}\uparrow$	$\boldsymbol{d_{z^2}}\uparrow$	$\boldsymbol{d_{xz}}\uparrow$	$\boldsymbol{d_{x^2}}\uparrow$	$\boldsymbol{d_{xy}}\downarrow$	$\boldsymbol{d_{yz}}\downarrow$	$\boldsymbol{d_{z^2}}\downarrow$	$\boldsymbol{d_{xz}}\downarrow$	$\boldsymbol{d_{x^2}}\downarrow$
$\boldsymbol{d_{xy}}\uparrow$	0	0	0	0	4	0	1	0	1	0
$\boldsymbol{d_{yz}}\uparrow$	0	0	0	1	0	1	0	3	0	1
$\boldsymbol{d_{z^2}}\uparrow$	0	0	0	0	0	0	3	0	3	0
$\boldsymbol{d_{xz}}\uparrow$	0	1	0	0	0	1	0	3	0	1
$\boldsymbol{d_{x^2}}\uparrow$	4	0	0	0	0	0	1	0	1	0
$\boldsymbol{d_{xy}}\downarrow$	0	1	0	1	0	0	0	0	0	4
$\boldsymbol{d_{yz}}\downarrow$	1	0	3	0	1	0	0	0	1	0
$\boldsymbol{d_{z^2}}\downarrow$	0	3	0	3	0	0	0	0	0	0
$\boldsymbol{d_{xz}}\downarrow$	1	0	3	0	1	0	1	0	0	0
$\boldsymbol{d_{x^2}}\downarrow$	0	1	0	1	0	4	0	0	0	0

Table S6. The calculated energy when the spin along different direction and magnetic anisotropy coefficient in $MnOCl_2$ monolayers with GGA + *U* method. The energy of [100] directions is taken as reference. The unit are all in the unit of μeV.

	001	100	010	110	K_y	K_z
Pmna	-9.25	0.00	-95.25	-48.25	42.33	4.11
Pmmn	-275.00	0.00	-228.50	-113.50	101.56	122.22

Table S7. The calculated magnetic moment for different atoms in $MnOCl_2$ monolayers with GGA + *U* method. The unit are all in the unit of μ_B.

	Mn1	Mn2	O	Cl1	Cl2
Pmmm	3.435	-	-0.305	-0.080	-0.080
Pmna	3.600	3.179	-0.287	-0.067	-0.066
Pmmn	3.732	3.727	-0.335	-0.061	-0.317